

Inhomogeneous magnetic cluster states in the magnetoresistance material $\text{Lu}_2\text{V}_2\text{O}_7$ K.-Y. Choi,¹ Z. Wang,^{2,3} P. Lemmens,⁴ H. D. Zhou,³ J. van Tol,³ N. S. Dalal,^{2,3} and C. R. Wiebe⁵¹*Department of Physics, Chung-Ang University, 221 Huksuk-Dong, Dongjak-Gu, Seoul 156-756, Republic of Korea*²*Department of Chemistry and Biochemistry, Florida State University, Tallahassee, Florida 32306, USA*³*National High Magnetic Field Laboratory, Florida State University, Tallahassee, Florida 32310-3706, USA*⁴*Institute for Condensed Matter Physics, TU Braunschweig, D-38106 Braunschweig, Germany*⁵*Department of Chemistry, University of Winnipeg, Winnipeg, Manitoba, Canada R3B2E9*

(Received 14 February 2010; revised manuscript received 28 June 2010; published 30 August 2010)

We report Raman scattering and multifrequency (54–336 GHz) electron-spin-resonance (ESR) measurements on $\text{Lu}_2\text{V}_2\text{O}_7$ single crystals in the temperature range 4–300 K with the view of understanding the origin of the large magnetoresistance in this lattice. The 307 cm^{-1} phonon mode undergoes a hardening at temperatures below $T_m=150\text{ K}$. Concomitantly, the single ESR peak arising from the paramagnetic V^{4+} ions becomes distorted. This is ascribed to the development of short-range magnetic correlations leading to a formation of magnetic clusters. Below the Curie temperature $T_C=70\text{ K}$ the ESR line develops with fine structures, indicative of an inhomogeneous ground state. Between T_m and T_C the magnetic cluster concentration decreases strongly as a function of the applied magnetic field, suggesting that the large magnetoresistance of this material could be due to the magnetic inhomogeneity in this lattice. The origin of what causes the initiation of such clusters is still unclear.

DOI: [10.1103/PhysRevB.82.054430](https://doi.org/10.1103/PhysRevB.82.054430)

PACS number(s): 75.47.Gk, 71.38.-k, 75.50.Dd, 76.30.-v

I. INTRODUCTION

Much effort has lately been devoted to investigations of colossal magnetoresistance (CMR) systems due to their fascinating physical properties as well as potential for technological applications.¹ Examples encompass a wide range of compounds: the perovskite manganites, the pyrochlore $\text{Tl}_2\text{Mn}_2\text{O}_7$ and the chalcogenide spinel FeCr_2S_4 .^{2–5} In the CMR manganites the magnetoresistance is largely explained within the double exchange (DE) interaction and electron-phonon coupling. In other materials, the CMR effects do not invoke DE and Jahn-Teller distortions because the magnetoresistance is not accompanied by structural anomalies. Rather, magnetic polarons are discussed as an underlying origin. According to the Majumdar-Littlewood model, the magnetoresistance in low-carrier-density ferromagnets depends on the carrier density, and for extremely low densities and large electron-core spin coupling, the carriers will self-trap into magnetic polarons.^{6,7} There are experimental indications that the pyrochlore compounds $\text{Tl}_2\text{Mn}_2\text{O}_7$ and $\text{Lu}_2\text{V}_2\text{O}_7$ are described by a polaronic scenario^{8,9} but additional details are desirable.

The vanadium pyrochlore $\text{Lu}_2\text{V}_2\text{O}_7$ has a face-centered cubic structure with space group $Fd\bar{3}m$. The crystal consists of a three-dimensional network of corner-sharing tetrahedra of V^{4+} ions. The compound undergoes a ferromagnetic transition at the Curie temperature $T_C\approx 70\text{ K}$.^{10,11} Polarized neutron diffraction and ^{51}V NMR studies evidence an orbital ordering where the half-filled vanadium $3d$ orbital is directed toward the center of the V tetrahedron.^{12,13} It is suggested that the orbital ordering leads to the ferromagnetic transition due to the energy gain through the hopping process from t_{2g} to e_g orbitals.¹⁴

The zero-field resistivity data exhibit typical semiconductor behavior while showing a drop between 60 and 75 K and a cusp around 75 K. This feature smears out in small mag-

netic fields. This points to a negative magnetoresistance, which reaches 50% at 75 K under an external field of $H=5\text{ T}$.⁸ The lattice parameters display no appreciable anomalies over the temperature range investigated. Only a tiny peak is observed in the thermal expansion coefficient around T_C due to the ferromagnetic transition. This seems to rule out any significant role of structural distortions in inducing the magnetoresistance. There are several hints for the formation of magnetic polarons for temperature below 160 K.⁸ For example, the magnetic specific heat starts to become anomalous around 160 K and the thermal conductivity is suppressed between 80 and 160 K. However, the resistivity is described by the Mott variable-range hopping model in the respective temperature interval. This is not compatible with the pure polaron conduction model. Rather, it indicates the presence of disordered, localized states.

In this study, we provide spectroscopic evidence for the presence of magnetic inhomogeneities in $\text{Lu}_2\text{V}_2\text{O}_7$. The analysis of the electron-spin resonance (ESR) and Raman spectra points to the formation of magnetic clusters around $T_m\approx 150\text{ K}$ and thus an inhomogeneous ground state. The magnetic clusters are proposed as a possible origin of the large magnetoresistance of this system.

II. EXPERIMENTAL DETAILS

Single crystals of $\text{Lu}_2\text{V}_2\text{O}_7$ were grown by the traveling-solvent floating-zone method.⁸ In an earlier study structural, magnetic, and transport properties of the crystals were extensively characterized by x-ray diffraction, superconducting quantum interference device magnetometry, resistivity, specific heat, and thermal conductivity.⁸ The presently reported Raman and ESR measurements were made on the same single crystal with dimensions of $2\times 2\times 1\text{ mm}^3$. High-frequency ESR experiments were performed at 240 GHz using the quasi-optical spectrometer that has been developed at

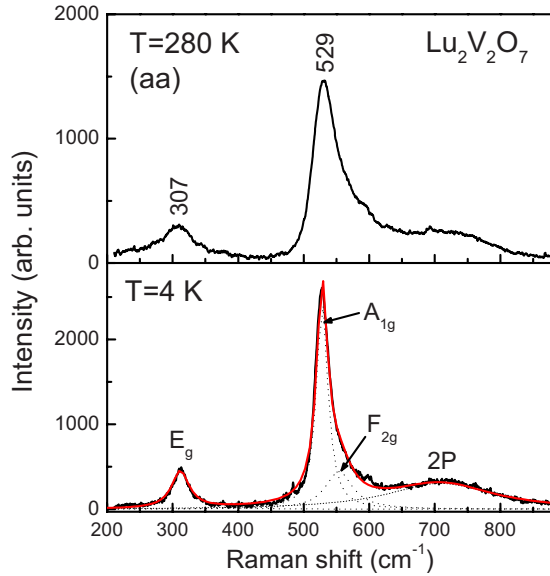


FIG. 1. (Color online) Representative Raman spectra of $\text{Lu}_2\text{V}_2\text{O}_7$ at $T=280$ K (upper panel) and at $T=4$ K (lower panel) in the (aa) polarization. The numbers denote the frequencies of the E_g and A_{1g} phonon modes. The F_{2g} mode appears due to a breakdown of the Raman selection rule. The 2P stands for two-phonon scattering. The dotted lines are a fit of the spectrum to a Lorentzian line and the solid line is the total sum of the four Lorentzian lines.

the NHMFL as well as at 54–336 GHz in a broadband transmission setup with a sweepable 15 T superconducting magnet.^{15–17} Raman-scattering measurements were carried out in a quasibackscattering geometry with the excitation line $\lambda=532$ nm of the Nd:yttrium aluminum garnet solid-state laser. An incident power of 7 mW was focused to a 0.1-mm-diameter spot on the [001] surface of the single crystal. Raman spectra were collected by a DILOR-XY triple spectrometer and a nitrogen cooled charge-coupled device detector.

III. RESULTS AND DISCUSSION

$\text{Lu}_2\text{V}_2\text{O}_7$ has a $Fd\bar{3}m$ (O_h^7) space group with eight formula units per unit cell. Factor group analysis yields six Raman-active modes; $\Gamma_{\text{Raman}}=A_{1g}(a^2+b^2+c^2)+E_g(2c^2-a^2-b^2)+4F_{2g}(ab, bc, ca)$. Figure 1 shows the Raman spectra of $\text{Lu}_2\text{V}_2\text{O}_7$ at 4 and 280 K in the (aa) polarization where the incident and scattered light are polarized parallel to the crystallographic a axis. Consistent with the group-theoretical analysis at room temperature we observe two pronounced peaks at 307 and 529 cm^{-1} . They are assigned to E_g and A_{1g} mode, respectively. The E_g mode corresponds to the rotation of VO_6 octahedra and the A_{1g} mode is due to the bending of VO_6 octahedra. Overall, the number and frequencies of the observed phonon modes are similar to those of the isostructural manganite pyrochlores $A_2\text{Mn}_2\text{O}_7$ ($A=\text{Ti, In}$).^{18,19} We note that there is a weak peak at the right shoulder of the 529 cm^{-1} mode. It is attributed to the F_{2g} mode, which is expected in cross polarizations. In addition, the weak, broad band denoted by 2P is observed in the higher-frequency

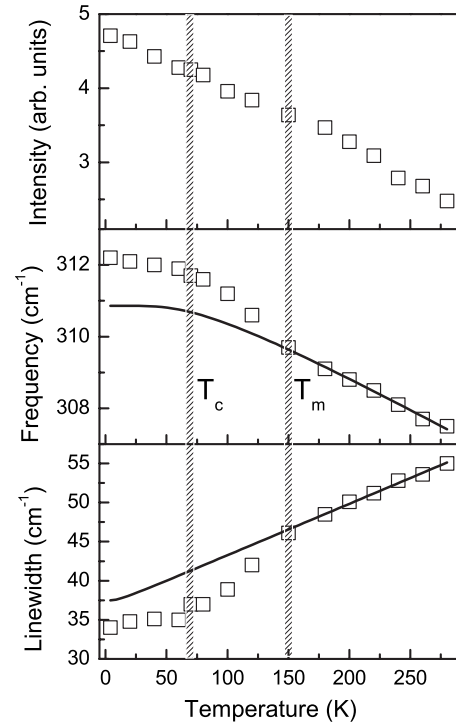


FIG. 2. Temperature dependence of intensity (upper panel), frequency (middle panel), and linewidth (lower panel) of the 312 cm^{-1} mode. The solid lines represent a fit to Eq. (1). T_C and T_m are the Curie temperature and the characteristic temperatures, see the text.

range of 550–880 cm^{-1} (see the dotted line in the lower panel of Fig. 1). Its frequency roughly doubles one-phonon scattering of the 307 cm^{-1} mode. Such a broad two-phonon scattering signal is reminiscent of two phonon density of states and might be related to defects and/or lattice inhomogeneities. This also accounts for a breakdown of the crossed polarization selection rule.

In order to analyze the temperature dependence of the phonon modes, the three phonon peaks and the two-phonon band are fitted to a sum of four Lorentzian profiles (see the dotted lines in Fig. 1). As in the manganite pyrochlores $A_2\text{Mn}_2\text{O}_7$, the A_{1g} and F_{2g} modes do not show any anomalous behavior.^{18,19} In the following, we thus focus on the E_g mode which shows a substantial change in the phonon parameters as a function of temperature. The temperature dependence of the 307 cm^{-1} mode is shown in Fig. 2. The errors are within a symbol size. With decreasing temperature the phonon intensity grows gradually and resembles the resistivity [compare with Fig. 3(a) of Ref. 8]. Its frequency undergoes a monotonic hardening by 5 cm^{-1} and the linewidth decreases continuously and becomes constant for temperature below T_C . On a qualitative level, these features seem to be consistent with lattice anharmonicities.

According to the Baltensperger and Helman model²⁰ a phonon frequency shift is proportional to the scalar spin correlation function: $\Delta\omega=\lambda\langle S_i \cdot S_j \rangle$, where λ is the spin-phonon coupling parameter. λ is proportional to the second derivatives of the coupling energy with respect to the atomic displacements. For ferromagnetic materials, the phonon shift is

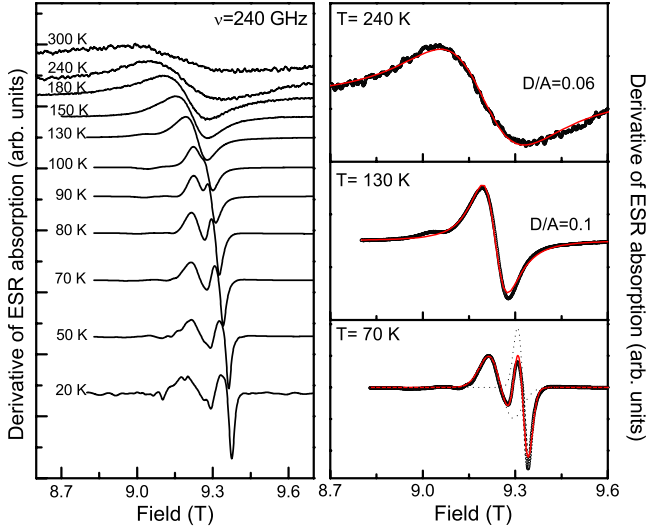


FIG. 3. (Color online) (Left panel) Temperature dependence of ESR spectra at 240 GHz. The external field is applied along one of the cubic crystal axes. The spectra are vertically shifted for clarity. (Right panel) Representative ESR spectra at $T=240$, 130, and 70 K. The dotted and solid lines are fitting curves. See the text for details.

related to the square of the magnetic moment of the magnetic ions.²¹ Actually, in the manganite pyrochlores $A_2Mn_2O_7$ the magnetic coupling mechanism leads to a hardening of the E_g mode below T_C .¹⁸

This motivates us to check carefully possible spin-phonon contributions to the observed frequency shift. As a first step, we estimated the anharmonic phonon contribution using a model based on phonon-phonon decay processes,²²

$$\omega_{ph}(T) = \omega_0 + C[1 + 2/(e^x - 1)], \quad (1)$$

where $x = \hbar\omega_0/2k_B T$. The fitting of the data over a whole temperature range does not give a satisfactory description (not shown here). As discussed above, phonons in magnetic materials can have complications due to an extra shift in an ordered state. Thus, the fitting interval is restricted to the high-temperature regime where a linear temperature dependence is observed. The fitted curve with the value of $\omega_0 = 310.9 \text{ cm}^{-1}$ and $C = -2.1 \text{ cm}^{-1}$ shows a clear deviation around $T_m = 150 \text{ K}$ which becomes stronger at lower temperatures (solid lines). This strongly suggests that there exists a spin-dependent phonon shift in addition to anharmonic lattice effects. In the manganite pyrochlores the hardening occurs below the magnetic-ordering temperature of T_C .¹⁸ In contrast, in the case of $\text{Lu}_2\text{V}_2\text{O}_7$, the deviation shows up at much higher temperature than T_C . Noticeably, the onset temperature, T_m , agrees well with the temperature of 160 K at which the thermodynamic and transport quantities show anomalies.⁸ This suggests that the phonon anomalies might be closely related to the development of magnetic correlations. To obtain a more detailed picture, we carried out ESR measurements.

Figure 3 displays the temperature dependence of ESR spectra taken at 240 GHz. The external field is applied along the a axis. At room temperature the ESR signal consists of a broad single line, which originates from paramagnetic V^{4+}

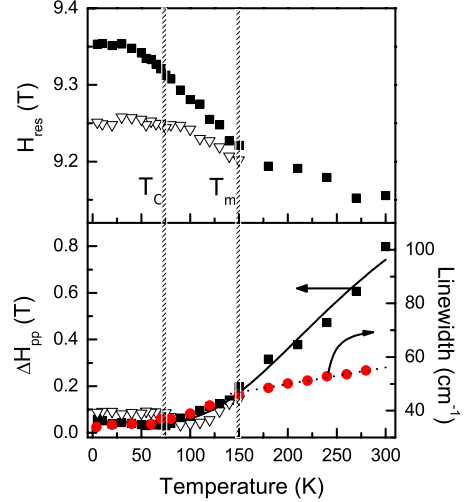


FIG. 4. (Color online) Temperature dependence of resonance field, H_{res} , (upper panel) and peak-to-peak linewidth, ΔH_{pp} (lower panel) from the spectra in Fig. 3. The vertical bars indicate the Curie temperature, T_C , and the characteristic temperature, T_m , related to the development of magnetic correlations. The phonon linewidth (full circle) is compared with the ESR linewidth (full square). The solid line represents a fitting curve by Eq. (2) and the dotted line is a guide for eyes.

ions. In order to differentiate skin depth effects, the ESR signals were fitted to a Dyson lineshape. We find that for $T > T_m$ the lineshape is close to pure Lorentzian, that is, the (D/A) ratio (admixture of absorption/dispersion of a Lorentzian line) is close to zero (see the right panel of Fig. 3). The Lorentzian shape implies that the signal is exchange narrowed and any contribution of the dispersion to the absorption is negligible. Upon cooling below T_m , the resonance line narrows and becomes distorted. It is not described by the Dyson lineshape anymore. Instead, the signal is largely approximated as a sum of two Gaussian lines as shown in the fit of the 70 K spectrum. This indicates that with decreasing temperature through T_m the relaxation-determined regime switches to the inhomogeneously broadened one. Below T_C the lower-field resonance develops a multiple-peak structure while the higher-field resonance stays a single Gaussian line. Because the sample is a high quality single crystal, we rule out the possibility of the inclusion of impurity phases. Further, the V^{4+} ions have negligible anisotropies of the g factor. Thus, the complex feature of the resonance suggests an inhomogeneous magnetic ground state where ferromagnetic and paramagnetic phases coexist. For the manganese perovskites the signals from the two phases are visible in the transition region.²³ In our case, however, they persist down to the lowest temperature. This might be due to the fact that our system is a low-carrier-density ferromagnet.⁸

Shown in Fig. 4 is the temperature dependence of the resonance field, H_{res} , and its peak-to-peak linewidth, ΔH_{pp} . Upon cooling down to 150 K, H_{res} displays a slight but almost linear change while ΔH_{pp} shows a strong and quite linear temperature dependence. At the respective temperature interval the 307 cm^{-1} phonon also shows a linear broadening. We note that in the high-temperature regime a linear T -dependent ESR line broadening was observed in the man-

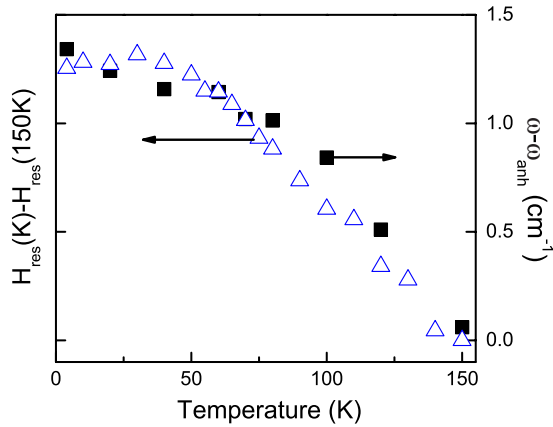


FIG. 5. (Color online) Comparison between the shift of $H_{res}(T)$ subtracted by $H_{res}(150\text{ K})$ (open triangle) and the phonon frequency shift subtracted by the estimated anharmonic contribution (full squares).

ganese perovskites and pyrochlores which has been discussed in terms of single-phonon spin-lattice relaxation and the bottlenecked spin-relaxation mechanism.^{24,25} This mechanism is unlikely for the studied system. Instead, we analyze $\Delta H_{pp}(T)$ in terms of the adiabatic small polaron hopping model²⁶

$$\Delta H_{pp}(T) = \Delta H_0 + (A/T)\exp(-E_a/k_B T), \quad (2)$$

where the second term is related to spin flips of charge carriers. In this model a line broadening is proportional to the hopping rate of the charge carriers, which limits the lifetime of a spin state. By fitting $\Delta H_{pp}(T)$ to Eq. (2) we obtain the activation energy $E_a = 61.8\text{ meV}$ (see the solid line of Fig. 4). This value measures the energy needed for the dissociation of the spin clusters. Between T_C and T_m H_{res} shifts substantially to higher fields and ΔH_{pp} decreases quasilinearly with a smaller slope ($d\Delta H_{pp}/dT$) than that for the high temperature. The lower-field signal (open triangle) shows a minimum linewidth at around 90 K. This is related to the development of short-range spin correlations. Below T_C both H_{res} and ΔH_{pp} exhibit a saturation. Remarkably, the phonon linewidth scales well with the ESR linewidth below 150 K.

In Fig. 5 we compare the spin-mediated phonon shift with the resonance field shift, $\Delta H_{res} = H_{res}(T) - H_{res}(150\text{ K})$. The former is obtained by subtracting the estimated anharmonic contribution (solid line in the middle panel of Fig. 2) from the phonon frequency (open squares in the middle panel of Fig. 2). Their evolution with temperature looks similar. Since the resonance field shift is associated with the development of internal magnetization, this gives further support to the spin-phonon mechanism of the phonon anomalies.

To understand the ESR behavior in the intermediate temperature regime we consider a competition of a narrowing relaxation process with a broadening mechanism. A line-narrowing mechanism is based on short-range magnetic correlations of spin clusters. The broadening is due to the increasing hopping rate of the charge carriers as the temperature is raised. As a result, the linewidth should display a minimum as can be seen in Fig. 4. Furthermore, we want to stress

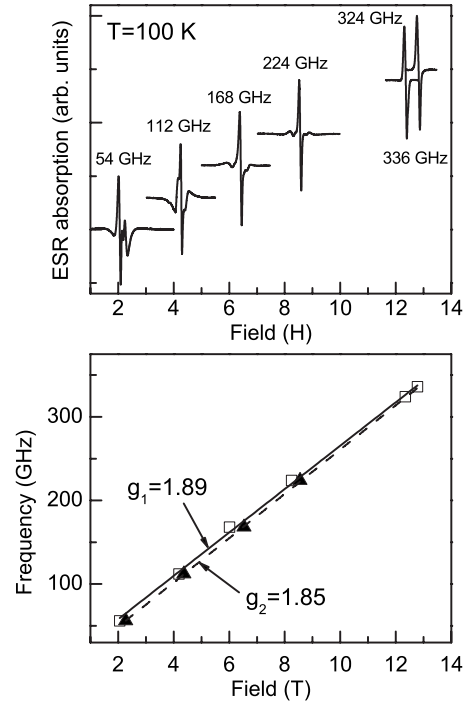


FIG. 6. (Upper panel) Frequency dependence of ESR signals at 100 K. (Lower panel) Frequency-field diagram of the two main ESR signals. Note that the intensity of the lower field peak decreases strongly at higher fields.

that the development of the inhomogeneous magnetic state itself can induce the change in the linewidth since the linewidth in a ferromagnetic single crystal is usually due to inhomogeneities in the demagnetization field.

We will now discuss the relevance of the magnetic polaron scenario to the studied compound. For a pure magnetic polaron system, a magnetic polaron is a regularly spaced ferromagnetic cluster containing one carrier. As long as there exist no magnetic correlations among the polarons, the system behaves like a superparamagnet.⁷ In this situation, the ESR signal is expected to be a single line, although the linewidth is narrowed by the polaron motion. In contrast, we observe the distorted ESR lines below T_m .

Furthermore, the substantial hardening of the 307 cm^{-1} mode, the persistence of the ferromagnetic cluster signal well below T_C , and the appreciable shift of the resonance field cannot be understood within a gas of magnetic polarons. Instead, ferromagnetic clusters form an inhomogeneous magnetic state. This suggests that our system is more complex than in the Majumdar-Littlewood model.^{6,7}

Figure 6 shows the frequency dependence of the ESR signals at $T = 100\text{ K}$. The linewidth does not show a significant frequency dependence. Possibly, the motional narrowing process competes with the single phonon mechanism at the temperature interval between T_C and T_m . With increasing frequency (field) the distortions with the multiple-peak feature fade away. This indicates that the binding energy of the magnetic clusters diminishes in an external magnetic field, suggesting an explanation of the negative magnetoresistance. In the lower panel of Fig. 6 we plot the frequency-field diagram of the two main signals. We find slightly different g -factors:

$g_1=1.89$ and $g_2=1.85$. This is consistent with the existence of ferromagnetic clusters in the paramagnetic matrix. The observed ESR peaks cannot be assigned to two different V^{4+} sites because then their relative intensities should be essentially independent of applied magnetic fields in contrast to the strong effect observed here (see Fig. 6).

However, the origin of the ferromagnetic clusters is less clear. For $Tl_2Mn_2O_7$, the hybridization among $Tl(6s)$, $O(2p)$, and $Mn(3d)$ orbitals leads to a formation of magnetic polarons.²⁷ In contrast, in the case of $Lu_2V_2O_7$ the Lu^{3+} ions do not provide extended s electron states. Thus, another mechanism needs to be invoked. One possibility is lattice inhomogeneities caused by oxygen deficient sites or/and regions where the orbital ordering is incomplete.¹⁴ The lattice inhomogeneities exert a pinning potential on the charge carriers which coalesce to form spin clusters. Extended x-ray-absorption fine structure experiments at the vanadium and oxygen edges are needed for clarifying this scenario.

To conclude, we have presented a combined ESR and Raman-scattering study of $Lu_2V_2O_7$, a compound known for its strong magnetoresistance whose mechanism is still not

understood. Both ESR and Raman spectra show anomalies at $T_m \approx 150$ K, which are ascribed to the formation of ferromagnetic clusters. The ferromagnetic clusters, embedded in a paramagnetic state, evolve into an inhomogeneous ground state. As expected for magnetic clusters, their binding energy decreased on the application of a magnetic field. The magnetoresistance in $Lu_2V_2O_7$ is not captured by a simple polaron model. A more realistic picture could be obtained by clarifying the cause of the magnetic clusters.

ACKNOWLEDGMENTS

K.Y.C. acknowledges financial support from the Alexander-von-Humboldt Foundation and the Priority Research Center Program funded by NRF (Grant No. 2009-0093817). Part of the work was supported by DFG, NSF, IHRP, and the EIEG program. A portion of this work was performed at the National High Magnetic Field Laboratory, which was supported by NSF Cooperative Agreement No. DMR-0654118, by the State of Florida, and the DOE. C.R.W. acknowledges support from NSERC of Canada.

-
- ¹E. Dagotto, *Nanoscale Phase Separation and Colossal Magnetoresistance* (Springer-Verlag, Berlin, 2003).
- ²E. Dagotto, T. Hotta, and A. Moreo, *Phys. Rep.* **344**, 1 (2001).
- ³M. A. Subramanian, B. H. Toby, A. P. Ramirez, W. J. Marshall, A. W. Sleight, and G. H. Kwei, *Science* **273**, 81 (1996).
- ⁴K.-Y. Choi, P. Lemmens, P. Scheib, V. Gnezdilov, Yu. G. Pashkevich, J. Hemberger, A. Loidl, and V. Tsurkan, *J. Phys.: Condens. Matter* **19**, 145260 (2007).
- ⁵A. P. Ramirez, R. J. Cava, and J. Krajewski, *Nature (London)* **386**, 156 (1997).
- ⁶P. Majumdar and P. B. Littlewood, *Nature (London)* **395**, 479 (1998).
- ⁷P. Majumdar and P. B. Littlewood, *Phys. Rev. Lett.* **81**, 1314 (1998).
- ⁸H. D. Zhou, E. S. Choi, J. A. Souza, J. Lu, Y. Xin, L. L. Lumata, B. S. Conner, L. Balicas, J. S. Brooks, J. J. Neumeier, and C. R. Wiebe, *Phys. Rev. B* **77**, 020411(R) (2008).
- ⁹B. Martínez, R. Senis, J. Fontcuberta, X. Obradors, W. Cheikhrouhou, P. Strobel, C. Bougerol-Chaillout, and M. Pernet, *Phys. Rev. Lett.* **83**, 2022 (1999).
- ¹⁰L. Soderholm and J. E. Greedan, *Mater. Res. Bull.* **17**, 707 (1982).
- ¹¹S. Shamoto, T. Nakano, Y. Nozue, and T. Kajitani, *J. Phys. Chem. Solids* **63**, 1047 (2002).
- ¹²H. Ichikawa, L. Kano, M. Saitoh, S. Miyahara, N. Furukawa, J. Akimitsu, T. Yokoo, T. Matsumura, M. Takeda, and K. Hirota, *J. Phys. Soc. Jpn.* **74**, 1020 (2005).
- ¹³T. Kiyama, T. Shiraoka, M. Itoh, L. Kano, H. Ichikawa, and J. Akimitsu, *Phys. Rev. B* **73**, 184422 (2006).
- ¹⁴S. Miyahara, A. Murakami, and N. Furukawa, *J. Mol. Struct.* **838**, 223 (2007).
- ¹⁵B. Cage, A. Hassan, L. Pardi, J. Krzystek, L. C. Brunel, and N. S. Dalal, *J. Magn. Reson.* **124**, 495 (1997).
- ¹⁶A. K. Hassan, L. A. Pardi, J. Krzystek, A. Sienkiewicz, P. Goyc, M. Rohrer, and L.-C. Brunel, *J. Magn. Reson.* **142**, 300 (2000).
- ¹⁷J. van Tol, L.-C. Brunel, and R. J. Wylde, *Rev. Sci. Instrum.* **76**, 074101 (2005).
- ¹⁸E. Granado, P. G. Pagliuso, J. A. Sanjurjo, C. Rettori, M. A. Subramanian, S.-W. Cheong, and S. B. Oseroff, *Phys. Rev. B* **60**, 6513 (1999).
- ¹⁹S. Brown, H. C. Gupta, J. A. Alonso, and M. J. Martinez-Lope, *Phys. Rev. B* **69**, 054434 (2004).
- ²⁰W. Baltensperger and J. S. Helman, *Helv. Phys. Acta* **41**, 668 (1968).
- ²¹E. Callen, *Phys. Rev. Lett.* **20**, 1045 (1968).
- ²²M. Balkanski, R. F. Wallis, and E. Haro, *Phys. Rev. B* **28**, 1928 (1983).
- ²³F. Rivadulla, M. Freita-Alvite, M. A. Lopez-Quintela, L. E. Hueso, D. R. Miguens, P. Sande, and J. Rivas, *J. Appl. Phys.* **91**, 785 (2002).
- ²⁴C. Rettori, D. Rao, J. Singley, D. Kidwell, S. B. Oseroff, M. T. Causa, J. J. Neumeier, K. J. McClellan, S.-W. Cheong, and S. Schultz, *Phys. Rev. B* **55**, 3083 (1997).
- ²⁵A. Shengelaya, G.-M. Zhao, H. Keller, and K. A. Müller, *Phys. Rev. Lett.* **77**, 5296 (1996).
- ²⁶A. Shengelaya, G.-M. Zhao, H. Keller, K. A. Müller, and B. I. Kochelaev, *Phys. Rev. B* **61**, 5888 (2000).
- ²⁷T. Saha-Dasgupta, M. De Raychaudhury, and D. D. Sarma, *Phys. Rev. Lett.* **96**, 087205 (2006).